SpaceLiner 8 definition: relevant aerodynamic and aerothermodynamic issues

Martin Sippel, Steffen Callsen, Jascha Wilken, Leonid Bussler, Sunayna Singh, Tommaso Mauriello
Martin.Sippel@dlr.de Tel. +49-421-244201145
Space Launcher Systems Analysis (SART), DLR, Bremen, Germany
Ysolde Prévereaud
ONERA, Toulouse, France

ABSTRACT

The SpaceLiner fully reusable launcher and ultra-high-speed rocket-propelled passenger transport is in conceptual design phase. The ongoing concept evolution is addressing system aspects of the next configuration release 8. The challenge of the passenger stage SLP8 design is to find an aerodynamic shape that allows both long-range glide missions with good hypersonic L/D, as in the case of current SpaceLiner 7, and ballistic jumps outside the atmosphere over populated landmasses.

The paper describes the latest architecture variation of the SpaceLiner 8 configuration still under definition. The focus is on the aerodynamic shape evaluation with search for trimmable designs in a very broad range of flight Mach-number and AoA.

Some of the trajectories reach up to 120 km altitude and are in the transition regime from continuum to rarefied flow. Hence, dedicated DSMC-calculations are performed for selected high altitude points of the trajectory and obtained coefficients are to be included into a refined AEDB and will subsequently be checked on system impacts. The aerothermal issues are investigated along different full mission profiles and suitable thermal protection concepts are preliminarily sized and evaluated.

Keywords: RLV, SpaceLiner, TSTO, aerodynamics, TPS, DSMC

Nomenclature

D	Drag	N
I_{sp}	(mass) specific Impulse	s (N s / kg)
L	Lift	N
M	Mach-number	-
T	Thrust	N
W	weight	N
g	gravity acceleration	m/s^2
m	mass	kg
q	dynamic pressure	Pa
v	velocity	m/s
α	angle of attack	-
γ	flight path angle	-

Subscripts, Abbreviations

AoA	Angle of Attack
BF	Body Flap
BL	Boundary Layer
CAD	Computer Aided Design
CFD	Computational Fluid Dynamics
DSMC	Direct Simulation Monte-Carlo
GLOW	Gross Lift-Off Mass
LEO	Low Earth Orbit
LH2	Liquid Hydrogen
LOX	Liquid Oxygen
MECO	Main Engine Cut Off
MRR	Mission Requirements Review
RLV	Reusable Launch Vehicle
SI	Structural Index
SL	SpaceLiner
SLB	SpaceLiner Booster stage
SLC	SpaceLiner Cabin
SLME	SpaceLiner Main Engine
SLO	SpaceLiner Orbiter stage
SLP	SpaceLiner Passenger stage
TPS	Thermal Protection System
TSTO	Two-Stage-To-Orbit
TVC	Thrust Vector Control
CoG	center of gravity
cop	center of pressure

1 INTRODUCTION

The key premise behind the original concept inception is that the SpaceLiner ultimately has the potential to enable sustainable low-cost space transportation to orbit while at the same time revolutionizing ultra-long-distance travel between different points on Earth. Manufacturing and operating cost of reusable launcher hardware should dramatically shrink by regular daily launches. Current routine operations of the SpaceX Falcon9 indicates the viability of this vision.

DLR's SpaceLiner concept is similar in certain aspects to the idea of multiple-mission reusable launch vehicles. These concepts are understood to serve quite diverse missions by the same or at least a similar vehicle. The most prominent example in this category is the SpaceX Starship&SuperHeavy [1, 2]. Recently, the Starship-launch vehicle [3] has achieved significant progress in its flight testing. While in its primary role conceived as an ultrafast inter-continental passenger transport, in its second role the SpaceLiner is intended as an RLV capable of delivering heavy payloads into orbit. Currently available simulations proof that the SpaceLiner orbital version stays within the load constraints of the PAX-version which confirms feasibility of the multiple mission intention.

First proposed in 2005 [4], the SpaceLiner is under constant development and descriptions of some major updates have been published since then [5, 6, 10, 12, 14]. The European Union's 7th Research Framework Programme has supported several important aspects of multidisciplinary and multinational cooperation in the projects FAST20XX, CHATT, HIKARI, and HYPMOCES. In the EU's Horizon 2020 program the project FALCon addressed the advanced return recovery mode "in-air-capturing" to be used by the reusable booster stage [7]. The way how such hypersonic point-to-point transports like SpaceLiner are to be integrated in future controlled airspace was addressed in the SESAR-project ECHO. The SpaceLiner has been one of the reference concepts

and its feasible intercontinental trajectories have been refined in dedicated analyses [21, 23].

At the end of 2012 with conclusion of FAST20XX the SpaceLiner 7 reached a consolidated technical status. An important milestone was reached in 2016 with the successful completion of the Mission Requirements Review (MRR) which allows the concept to mature from research to structured development [6]. The Mission Requirements Document (MRD) is the baseline and starting point for all technical and programmatic follow-on activities of the SpaceLiner Program. In the same year the unmanned orbital stage (SLO) for cargo transport to space has been defined [6], making the concept a fully reusable TSTO to LEO.

This paper does not intend on providing a complete technical overview of the SpaceLiner, but instead focusing on recent aerodynamic and aerothermal analyses. More extensive overviews on the latest SpaceLiner technical definition including descriptions of the SpaceLiner 7's consolidated technical status have been published in references 20 and 21.

The parallel arrangement of SL7's two reusable vehicles at lift-off is presented in e.g. references [6, 20, 21]: a large unmanned booster stage and a passenger or orbital upper stage. All 11 SLME engines are operating right from lift-off, 9 on the booster and 2 on the upper stage which is fed by propellant crossfeed in the mated section of the flight. External shapes of passenger and orbital configuration with satellite payload are almost identical. This approach intends enabling dramatic savings on development cost and moreover by manufacturing the vehicles on the same production line, also significantly lower hardware cost than would result for a dedicated new lay-out [6]. The internal arrangement of the upper stage is adapted to the specific mission with either a forward passenger cabin or a central cargo bay and adequately placed LOX-tank (see [6, 20]). The main dimensions of the 7-3 booster configuration and passenger or orbiter stage are summarized in [20, 21].

1.1 Preliminary shape and size of SL8

The partially modified, potential lay-outs of the SpaceLiner 8 are shown in Figure 1 for the booster (SLB) and in Figure 2 for the reusable upper stage. Note, the configurations as visible do not yet represent a converged updated design but serve further refinement of subsystems or improvement of safety or mission performance. Some of these aspects are addressed in the subsequent chapters 2 and 3. The baseline assumption of both stages being arranged in parallel during lift-off is unchanged in order to keep the overall length of the launcher in manageable size and continue propellant crossfeed between booster and upper stage.

For the SLB 8 a deployable outer-wing option (Figure 1) has been checked on integration and mass impact [12]. A partially automatic variation of parameters was implemented in an MDA approach in order to systematically search for feasible and promising lay-outs shown in [12]. Instead of trailing edge flaps the inner segment had separate spoilers on its lower and upper surface.

In the Iteration 3 of the SLB8 V3 design it has been decided to add an additional, 10th rocket engine to improve thrust-to-weight ratio at lift-off, thus, reducing gravity losses with almost similar ascent propellant mass compared to SLB7-3. The fuselage diameter is increased to 8.8 m. As a consequence, the stage length reduces to 79.1 m. Span with deployed outer segment reaches 53.8 m while the span of retracted wing is reduced to merely 28.8 m.

The upper stage has been subjected to an intensive shape variation and optimization process of the wing described in detail in [18, 19]. The fuselage of the preliminary variant O40-0042 (Figure 2) remains unchanged to SLP7 while the wing span and its overall surface have been significantly reduced. An adaptation also of the fuselage is likely but requires as first step the selection of a promising new design of the passenger capsule (SLC) [14, 21]. Recent results of ongoing systematic investigations for improving the aerodynamic characteristics of the SLC are reported in [24].

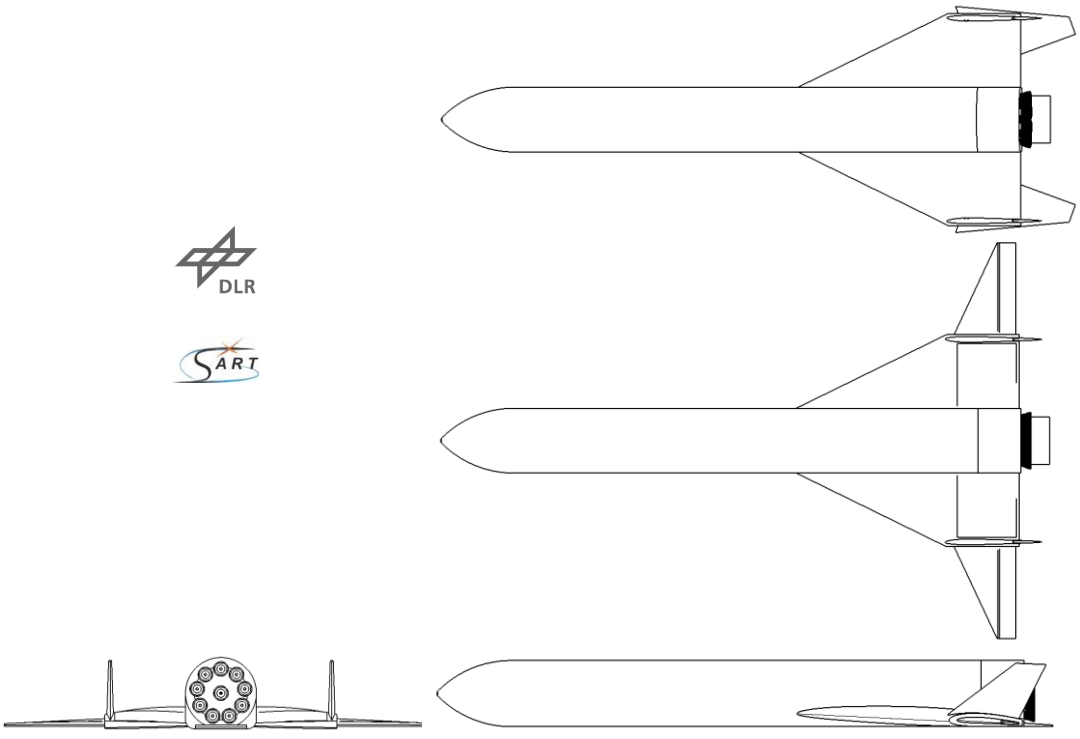

Figure 1: Drawing of preliminary SLB8 variant V3 It. 3 with sweep-wing in stored (top) and deployed (center) position

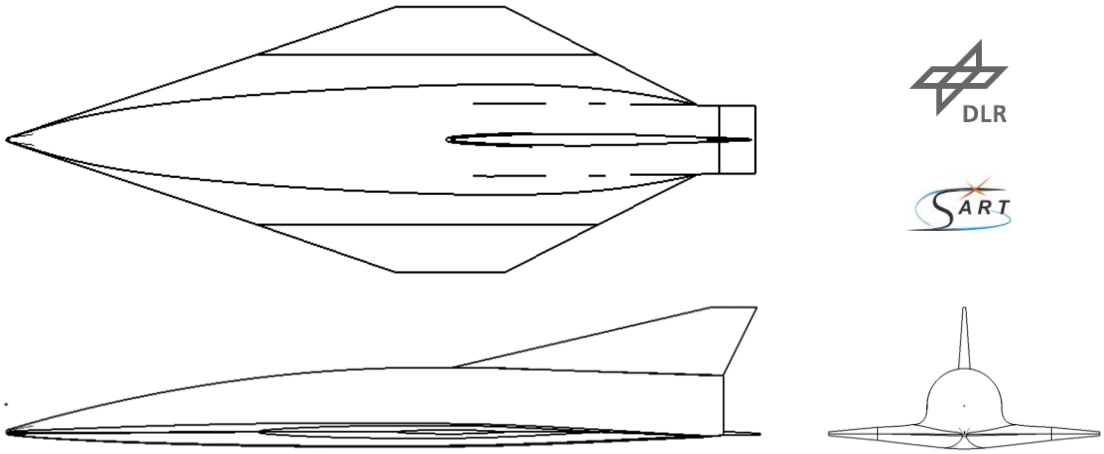

Figure 2: Drawing of preliminary SLP8 variant O40-0042

1.2 Main propulsion system

Staged combustion cycle rocket engines with a moderate 16 MPa chamber pressure have been selected as the baseline propulsion system right at the beginning of the project [4]. A Full-Flow Staged Combustion Cycle with a fuel-rich preburner gas turbine driving the LH2-pump and an oxidizer-rich preburner gas turbine driving the LOX-pump is the preferred design solution for the SpaceLiner [6]. The expansion ratios of the booster and passenger stage/orbiter engines are adapted to their respective optimums; while the mass flow, turbo-machinery, and combustion chamber are assumed to remain identical in the baseline configuration.

The SLME has the requirement of vacuum thrust up to 2350 kN and sea-level thrust of 2100 kN for the booster engine and 2400 kN, 2000 kN respectively for the passenger stage. Data of the nominal operational MR-range from 6.5 to 5.5. are listed in [13, 21].

The size of the SLME in the smaller booster configuration is a maximum diameter of 1800 mm and overall length of 2982 mm. The larger passenger stage SLME has a maximum diameter of 2370 mm and overall length of 3893 mm. A size comparison of the two variants is shown in e.g. [20] and the current arrangement of the engine components is published in [13]. All engines have a 2D TVC capability, electro-mechanically actuated.

The engine masses are estimated at 3500 kg with the large nozzle for the passenger stage and at 3218 kg for the booster stage. These values are equivalent to vacuum T/W at MR=6.0 of 65.9 and 69.7. Some optimization potential exists, mainly with elimination of high-pressure LOX-lines by introducing an advanced annular ox-rich powerhead [13].

1.3 Launcher system masses

Based on available subsystem sizing and empirical mass estimation relationships the booster and passenger stage masses are derived. The SpaceLiner 7-3's GLOW reaches about 1832 Mg for the reference mission Australia – Europe while the TSTO is at 1807 Mg (compare e.g. [20, 21]) still below that of the Space Shuttle STS of more than 2000 Mg.

The SpaceLiner 8 might see a slight increase in GLOW, although, any real assessment is too early before the designs are consolidated. The component-level mass estimations allow for a relatively accurate calculation of the CoG-positions.

2 PRELIMINARY AERODYNAMIC DESIGN OF SPACELINER 8

The architecture variation of the SpaceLiner 8 configuration is still ongoing. The aerodynamic shape evaluation is primarily governed by the search for trimmable designs in a very broad range of flight Mach-number and AoA as already considered for SpaceLiner 7 [10]. The SL8 designs are more demanding because additional aspects are to be integrated: The biplane architecture of the mated launch configuration (shown in e.g. [6, 12, 14, 20, 21]) is problematic because of complex high-speed flow interactions of the two stages during ascent flight. Both, the complicated flow of the launch configuration and shock-shock interaction during booster reentry have motivated the investigation of potential geometry changes and improvements to the SpaceLiner booster wing geometry. Further, the passenger stage should not only achieve good hypersonic L/D (as with SLP7 [10]) but also should be capable of reentry with elevated AoA while fully trimmable. Therefore, a compromise has to be found enabling good mission performance for multiple connections [18, 19, 21].

Some of the new point-to-point trajectories of SL8 reach almost up to 120 km altitude [19, 21].and are in the transition regime from continuum to rarefied flow. Hence, dedicated DSMC-calculations are to be performed for selected high altitude points of the trajectory and obtained coefficients are subsequently to be checked on system impacts as achievable range or heatflux.

Although, the study for the next SpaceLiner 8 design targeting major improvements is ongoing without yet any downselection performed, important intermediate results of its aerodynamic definition are presented in the following sections.

2.1 SLB8

In order to reduce biplane flow interactions during ascent and to avoid the shock-shock-interaction on the outboard leading edge, a drastically reduced size of the SLB wing had been investigated as a first proposal for the Booster, called SLB8V2. Such a small wing will not be sufficient for horizontal landing of the RLV-stage. L/D is also not satisfactory to allow the tow-back using the "in-air-capturing"-technique. Consequently, the SLB8V2 would need to be designed for vertical downrange landing on a sea-going ship, not compliant with the preferred operational model.

As the vertical landing SLB8V2 turned out to be not fully convincing, alternative designs have been explored [12]. It has been tried to maintain the promising hypersonic aerodynamic configuration with small fixed wings, however, in order to allow the stage to use "in-air-capturing" [7] and horizontal landing, deployable wing options have been checked on integration and mass impact [12]. The challenge of this design is finding a suitable combination of different wing shapes which achieve a sufficiently high trimmed subsonic L/D, acceptable landing speed but also being fully trimmable in hypersonic flight at high-angles of attack.

A partially automatic variation of parameters was implemented in a multi-disciplinary design analysis (MDA) approach including subsonic as well as hypersonic aerodynamics, structural predesign and mass estimation and reentry flight dynamics. The systematic search for feasible and promising lay-outs is described in [12].

A variable sweep wing configuration has been studied for SLB8-V3 which in its stored position is only partially protected by the fixed segment and the tip section extending backwards (Figure 1, top). This might be a useful feature for the generation of lift at the vehicle's aft end supporting hypersonic trim requirements. The SLB8-V3 includes an inner fixed part of the wing comparable in size and geometry to the V2 which itself generates sufficient lift in hypersonic, high AoA flight. Bow-shock interaction with the outboard leading edge can be avoided and biplane flow effects during ascent are reduced.

The integration of the outer wing segment inside the inner part is essential for the technical feasibility and has been preliminarily analyzed in CAD [12]. The connecting and pivot-point of the outer part is positioned behind the leading-edge box close to the maximum thickness of the fixed inner airfoil. The trailing edge of the inner part is kept open to allow the sweeping part to be stored. Consequently, instead of trailing edge flaps the inner segment has separate spoilers on its lower surface.

A map of L/D-ratios calculated with surface inclination method in the broad range of Mach-numbers 4 to 13 and AoA from -5° to 45° is shown under fully turbulent assumption in Figure 3. A significant positive spoiler and bodyflap deflection of around 10° and 20° would be required to reach roughly a trimmed state. Then the configuration is neutral or marginally stable at best with some uncertainty on the actual pressure distribution due to a strong separated shock in front of the vehicle in case of high AoA-flight.

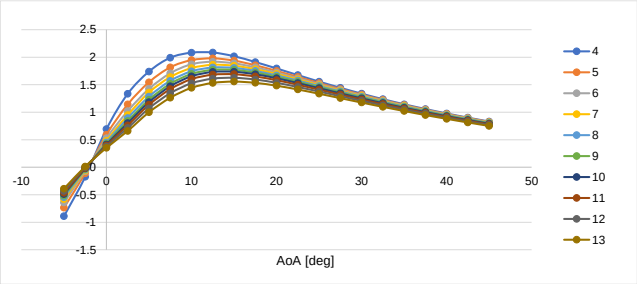

Figure 3: Calculated hypersonic L/D ratio of SLB8 V3, spoiler deflection angle η= 10°, BF deflection 20°

In the lower supersonic flight regime and in the subsonics the SLB8 should be operated with the outer wing segment fully deployed (Figure 1, center). In an early assessment of the subsonic characteristics, empirical estimation methods have been used. Assuming at the time of analyses [22], a negative (upward) spoiler deflection η of -11° on the main wing could reach a pre-trimmed state with the bodyflap neutral. The maximum L/D ratio might be around 6 at Mach numbers below 0.5 and AoA of 10° (Figure 4). At higher angles of attack the wing might encounter flow separation and, hence, this region is to be avoided.

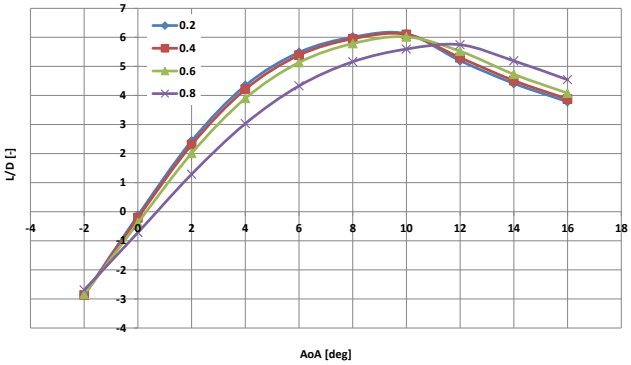

Figure 4: Calculated trimmed, subsonic L/D ratios of SLB8 V3 with assumed negative spoiler deflection on wing upper side [22]

Pre-trim calculations based on the empirical aerodynamic methods should be treated with some caution. Therefore, the SLB8 V3 had been analyzed in subsonics at selected flight points also using the OpenFOAM (OF) tool under inviscid assumptions. In Figure 5 the obtained lift-to-drag ratios are compared to the empirically based calculation (CAC). Lift-curve slope is found very similar by both methods [22]. The drag coefficient values in this example are based in both cases on empirical relations. Under these circumstances, the CFD results deliver glide ratios of not more than 5.0 at the angles of attack 10° and 14°.

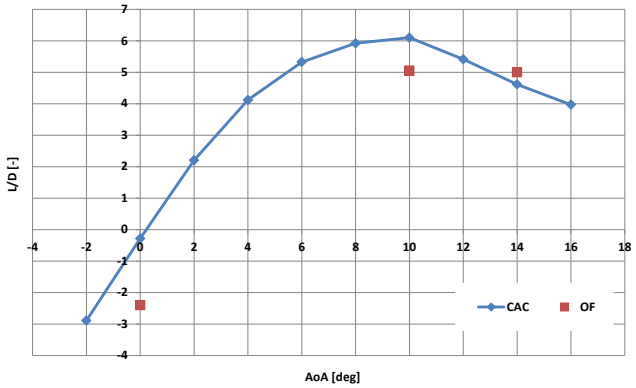

Figure 5: Comparison of CFD-derived and empirically calculated L/D ratios of SLB8 V3 at Mach 0.5 [22]

The somehow sobering results demonstrate the challenge of achieving improved trimmed L/D in subsonic flight which, however, is essential for making the "in-air-capturing" recovery of the heavy RLV with empty weight above 200 tons feasible with existing aircraft. As this requirement is not fulfilled with the SLB7 [21], further improvements are to be investigated or alternative recovery solutions to be implemented. Trim behaviour in hypersonics could be enhanced with shorter fuselage of increased diameter. The SLB8-V3, nevertheless, is useful for evaluating integration of advanced TPS (section 3.1 below) and testing different aerodynamic shapes. A converged SpaceLiner 8 booster is likely to have significantly different shape to the one shown in Figure 1.

2.2 SLP8 / SLO8

Even more than the booster, the upper stage has been subject to extensive MDAO of its wing position and planform [18, 19] while its fuselage's external surface and internal tank arrangement was left untouched in the first step. The passenger capsule CoG-assumptions are already considering the baseline modifications of SLC8 as explained in [20, 21]. Later, more radical changes of the

SLC [24] are unlikely to be compatible with the SLP7 fuselage and together with different tank lay-out will see another, possibly more radical MDAO-loop in the future.

Figure 6 shows a direct comparison between the wing planform of the preselected SLP8 variant O40-0042 with respect to the SLP7. The major reduction in wing area is obvious. The SLP8 candidate has more forward-shifted wings, which provide better trim performance (improved relative position between the CoG and the hypersonic cop). In fact, this vehicle can generate more lift at hypersonic velocities than the SLP7 despite its smaller wings as it is trimmable up to at least 40° of angle of attack at reference Mach number 14 (while the SLP7 only up to 28°). [19]

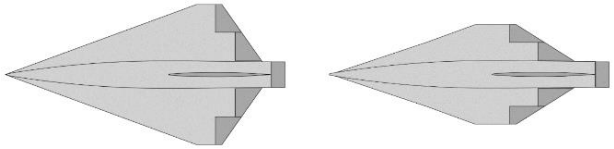

Figure 6: Comparison between wing planform geometries of SLP7 (left) and SLP8 candidate (right) [19]

The SLP8 variant's aerodynamic performance in high-speed flight remains impressing despite the assumptions of reduced wing size but untouched fuselage compared to SLP7 (of which selected data was published in e.g. [10]). The map of L/D-ratios calculated with surface inclination method in the very broad range of Mach-numbers 4 to 28 and AoA from -4° to 44° is presented in Figure 7. The supposed deflections of the data in this plot are close to achieve longitudinally stable, trimmed conditions at angles of attack of around 40°. Following a typical flight profile, the boundary layer transition occurs below Mach 14 and 58 km while above the BL is assumed as staying mostly laminar.

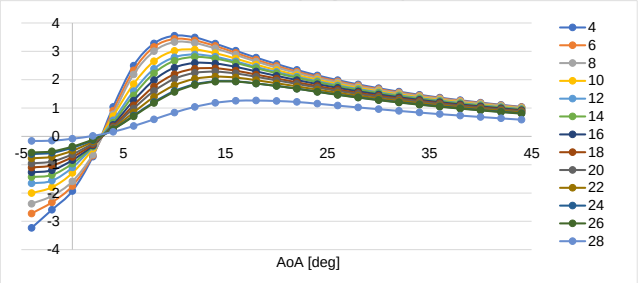

Figure 7: Calculated hypersonic L/D ratio of SLP8 variant O40-0042, flap deflection angle η= -20°, BF deflection -10°

The landing speed subsonic aerodynamics need to be considered to confirm practical feasibility of the much smaller size wing in the full flight regime. Inviscid Euler calculations with OpenFOAM have been used to check preliminary MDAO-results based on empirical relations. Subsonic flow conditions of the SLP8 variant O40-0042 at landing approach speed of Mach 0.3 are presented in Figure 8. A leading-edge vortex on the upper surface being typical for delta wings under such environments is clearly visible. These vortices are responsible for the additional lift at high AoA conditions and have an important effect on surface pressure distribution and hence pitch moment coefficient c_M [21]. For two analyzed flap deflections of 10° and 25° the trimmed state is reached for AoA of 7.5° and 13° respectively. This corresponds to landing speeds of 98 m/s and 71 m/s assuming a typical landing mass of 122 t. [19], both compliant with the speed limit set to 100 m/s. The SLP8 variant O40-0042 is longitudinally unstable in subsonics under the current estimation of its likely CoG-position.

The MDAO-process of the aerodynamic configuration of SLP8 has been very successful with variant O40-0042 showing promising characteristics and being feasible in the complete flight regime. Nevertheless, the SLP8 is not yet frozen because the fuselage might see major adaptations due to an update of the capsule and different propellant loading and hence different tank lay-out.

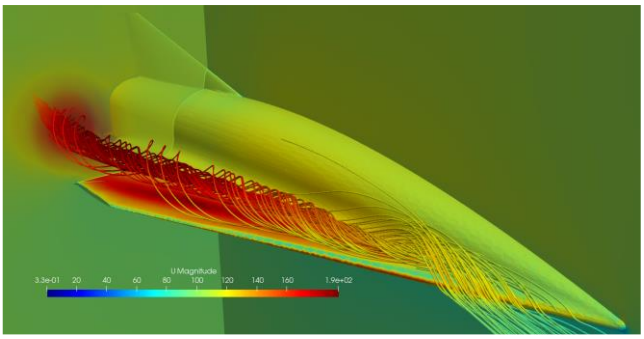

Figure 8: Computed flow field on SLP8 variant O40-0042 in subsonics close to landing conditions (M= 0.3 / AoA = 20°)

2.3 SLP8 in rarefied flow regime

At high altitude, the wall heating is generally very low compared to the one encountered in continuum regime and is thus non-dimensioning for the system. However, to assess the flying quality and ensure a correct trajectory prediction, the aerodynamic force and moment coefficients must be predicted for the whole flight, from the take-off to the landing.

The best adapted numerical approach (CFD or Direct Simulation Monte-Carlo (DSMC)) to simulate the flow must be chosen in function of the Knudsen number Kn, which describes the rarefaction level of the flow. The Knudsen number is defined as the ratio between the molecular mean free path length and a reference length L_{ref}. According to the selected reference length, the Kn value can be significantly different. For the passenger stage SLP, the nose radius s around 0.2 m, while the total length of the vehicle is 65 m. In this case, two radically different Knudsen numbers indicate different levels of rarefaction of the flow at a given altitude, as illustrated in Table 1.

Table 1: Flight points under investigation for SLP8 ballistic arcs and corresponding Kn-numbers

Altitude (km)	Mach number	Kn (L_{ref} = 65 m)	Kn (L_{ref} = 0.2 m)	AoA (°)
108.13	25.30	8.74×10^{-3}	2.84	22.3
102.14	26.82	3.15×10^{-3}	1.02	8.7
101.42	26.93	2.79×10^{-3}	0.91	31.8

The flow is considered to be in a continuum regime when Kn < 0.001. When 0.001 < Kn < 0.1, the gas is in a slip flow regime and transitional non-equilibrium is important only near the surfaces. Finally, the regime is said to be transitional for 0.1 < Kn < 10. In this regime, intermolecular collisions effects start to be significant, but not enough to reach a local equilibrium. In continuum regime, Navier-Stokes codes are used to simulate the flow. In slip flow regime, DSMC or CFD simulations with slip boundary conditions at the wall should be employed. In other cases, Navier-Stokes conservation equations are no more valid and particle methods, as DSMC, must be used.

The numerical simulations of SLP8 to be performed in the rarefied flow conditions of Table 1 are very challenging:

- The flow around the SLP is expected to be in thermo-chemical non-equilibrium, having between 5 (O_2, N_2, O,

N, NO) and 11 gas species (O_2, N_2, O, N, NO, O_2^+, N_2^+, O^+, N^+, NO^+, e^-);

- The vehicle size leads to the generation of large meshes, with a minimum of 50 million elements, requiring substantial CPU-times;
- Due to the geometric characteristics of the vehicle, the flow can be locally rarefied or continuous, leading to uncertainty about the appropriate numerical method to be used;
- The Navier-Stokes and DSMC methods are within their limits of application in the flow regimes considered if L_{ref} = 65 m is considered to calculate the Knudsen number. The two methods may both be used in this case, but at the expense of huge CPU-times and still uncertainties on the obtained results.

In a preliminary investigation, both CFD and DSMC simulations are in progress for the 2nd flight point (102 km; Mach 26.82; α = 8.7°). For the DSMC-simulations, the computational domain was defined as a large box whose size is sufficient to ensure that the freestream conditions can be imposed at the inlet and supersonic conditions are reached at the outlet. The surface mesh used for our simulation and realized with CENTAUR is illustrated in Figure 9.

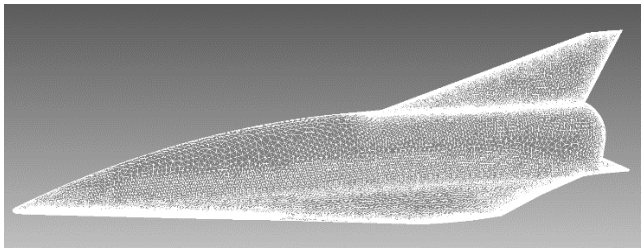

Figure 9: SLP8 surface mesh with 393,458 elements for DSMC-simulation

For the CFD-computation, the volume mesh generated with CENTAUR is shown in Figure 10. These 3D unstructured meshes are composed of prismatic and tetrahedral cells. The exact position of the shock is captured in a highly refined zone, composed of prismatic layers. To properly capture the gradients at the wall, prismatic layers have been prescribed near the wall: the size of the first cell being 1 µm with a stretching ratio of 1.2.

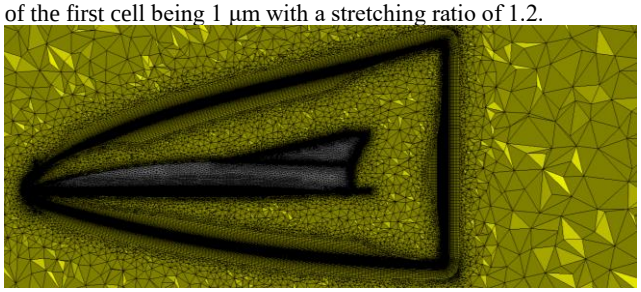

Figure 10: SLP8 surface and volume mesh with more than 50 million elements for CFD simulation

3 AEROTHERMAL ANALYSES AND THERMAL PROTECTION SYSTEM

The aerothermal issues have been investigated along different full mission profiles and suitable thermal protection concepts are preliminarily sized and evaluated. DLR-SART has been using its significantly improved TPS-system sizing tool *TOP* in version 3 which is optimizing the insulation layer in 1D- heat conduction analysis of user-defined material stacks for individual surface temperature ranges. A new feature of the tool is a quasi-coupled simulation, iterating the external temperatures of the TPS while also considering the heatflux into TPS and underlying structure. The insulation thickness is adapted such that a preset limit temperature of a selected internal layer is never exceeded during the mission.

3.1 SLB8

Selection of suitable TPS materials requires the knowledge of the surface temperature distribution which is calculated for the classic adiabatic equilibrium case. However, this computation is not only done for a single flight point (e.g. at maximum stagnation point heatflux) but along the full mission trajectory. The rapidly changing AoA-history in critical parts of the mission is taken into account and thus the actual dimensioning maximum temperatures are considered, not necessarily all reached at the same flight condition. Figure 11 shows the expected equilibrium temperature distribution of SLB8 with almost 2000 K in the small leading-edge area and on the deflected spoiler on the lower side of the wing and on the bodyflap. Large areas on the upper side of SLB8 see maximum temperatures not exceeding 400 K to 600 K.

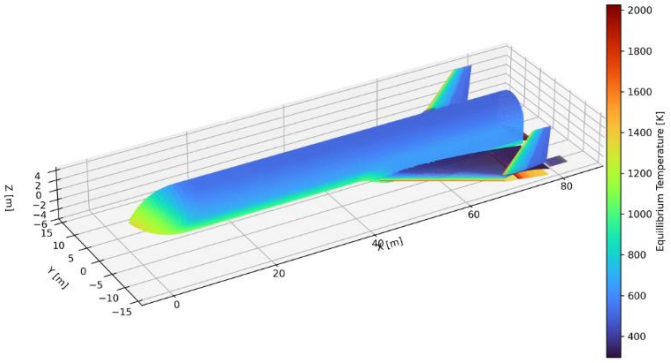

Figure 11: Calculated dimensioning equilibrium temperatures on SLB8 V3 external surface shown in reentry configuration

A critical aspect for RLVs like the SpaceLiner is the selection of reusable cryogenic tank insulation which works under multiple environmental conditions. Independent of weather conditions (e.g. temperature, humidity) effective insulation needs to be ensured and icing on the vehicle external surface is to be avoided. DLR has performed systematic research on promising combinations of insulation and reentry TPS for which the SLB7-3 served as the reference system concept. The booster stage's reusable cryogenic tank insulation has been investigated under consideration of the external TPS by numerical simulation and ground experiments [16, 17].

The pre-selected design option includes a so-called purge gap creating a distinct gap between the insulation of the cryogenic tank and the external thermal protection system, which has to be resistant to temperatures beyond typical limits of cryo-insulations. This relatively complex combination of external TPS and cryogenic insulation has been selected in order to avoid icing even in humid and relatively cold environment. In the gap a forced flow of pre-heated dry gas is providing a controlled boundary condition at the outer interface of the cryogenic insulation. A description of the purged insulation for metallic integral cryogenic tanks on RLV is publicized in [16, 17].

Numerical and experimental results from the DLR projects AKIRA and TRANSIENT demonstrate the reusable insulation concept is functioning [16, 17], however, a mass impact on the SLB stage is expected compared to earlier SLB7 suppositions. This effect is due to the increased weight per surface area but also by the reduced available volume for propellants inside the SLB

because of the enlarged thermal protection thickness compared to the previous assumptions.

At the end of the AKIRA-project the newly defined purge-gap TPS has been applied to the SLB8 V3-variant. A TPS with external metallic surface (either Inconel or Titanium or Aluminum depending on the expected maximum temperatures) has been assumed. The preliminary TPS type distribution of SLB8 is shown in Figure 12. Almost the complete fuselage is protected by the metallic TPS with gap. The only exception is the nose cone which is a separate structure ahead of the forward LOX-tank dome. The wing, fin, spoiler and flaps have a more classical TPS-lay-out. The upper side of the wing could be sized as metallic hot-structure with large areas not requiring insulation. The lower side of the wing and in particular the deflected spoiler and bodyflap experience most of the heatloads and could reach temperatures close to 2000 K for short periods. Ceramic materials are to be selected. In case of spoiler and bodyflap, probably no major insulation layer will be required with CMC supported by steel frames on the leeward side. Detailed investigations of this concept have not yet been performed.

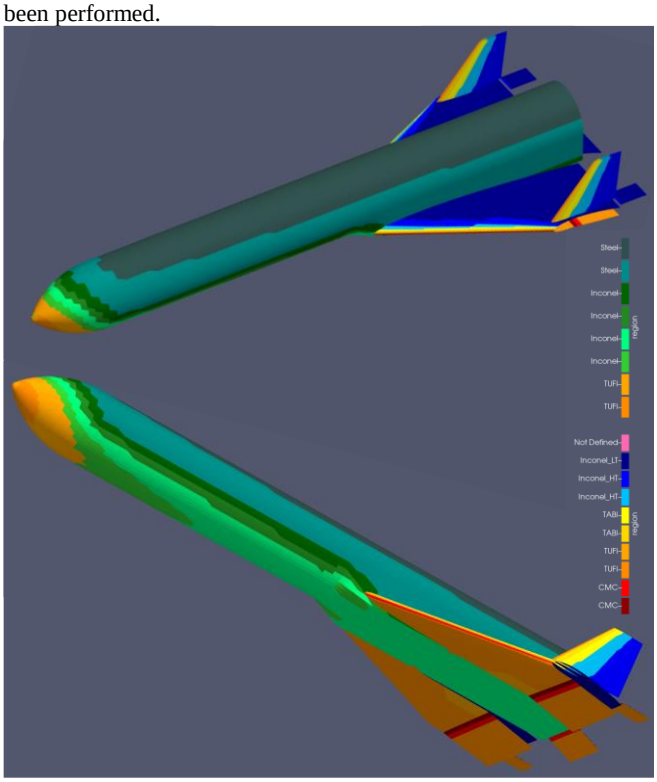

Figure 12: TPS-type distribution on SLB8 V3 in views of top and bottom side

3.2 SLP8 / SLO8

The external thermal protection has also been preliminarily defined for the SLP8 following the SL7 pre-selection (e.g. [9, 11]). Figure 13 shows the TPS distribution on the upper and lower surface based on selected SL8 reference trajectories and subsequent iterative sizing. The windward side is protected by CMC with variable insulation thickness in the internal layers while for the upper surface TABI or AFRSI has been selected similar to the Space Shuttle.

A small area at the nose and leading edges including the fin needs active cooling and is labeled “Not defined” in Figure 13. This actively cooled section has been an important element of the SpaceLiner concept since the early days of the vision [5]. Different cooling ideas have been evaluated and tested in windtunnel conditions with focus on transpiration methods in the beginning. An overview on the active cooling types considered for the SpaceLiner is found in [11, 15].

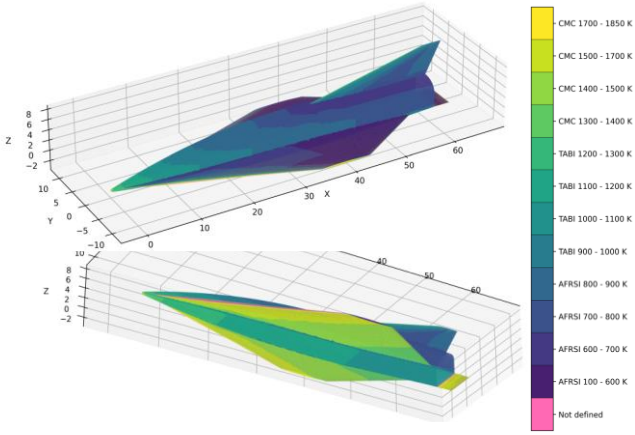

Figure 13: Preliminary distribution of TPS-types on SLP8 variant O40-0042 in views of top and bottom side

4 CONCLUSION

The DLR proposed reusable winged rocket SpaceLiner for very high-speed intercontinental passenger transport is progressing in its conceptual design phase. Research activities have shifted towards the next configuration level 8 with the ambition to address remaining open critical points. Both stages of the TSTO are under redesign evaluation. Results of promising concepts in the field of aerodynamic and aerothermodynamic behavior are summarized.

A key target for both new stages is the reduction of wing size while at the same time keeping essential characteristics of the SpaceLiner 7. This approach should reduce vehicle dry masses and at the same time minimize the flow interactions between the stages in parallel arrangement during mated ascent.

The large unmanned booster stage (SLB) has been studied with a partially sweep-wing design. The movable outboard wing segments are stored during ascent and in hypersonic reentry and would be deployed in the lower speed regime. Although this concept is showing some promising features, the trim characteristics in high-speed flight and the achievable glide ratios in subsonic flight are not yet satisfactory. Further, on the downside, the mechanical architecture of the large movable elements will add dry mass.

The upper or passenger stage (SLP) has been subjected to an extensive MDAO-process delivering an aerodynamic configuration showing very promising characteristics and being flyable in the complete operational regime. Nevertheless, also the SLP8 might see major adaptations in the future due to an update of the passenger capsule and different, refined tank lay-out.

The SpaceLiner 8 definition is not yet completed but technically and operationally promising approaches are identified and major steps forward are evident.

5 ACKNOWLEDGEMENTS

The authors gratefully acknowledge the contributions of Ms. Carola Bauer, Ms. Mona Carlsen, Ms. Elena Casali, Ms. Nicole Garbers, Ms. Carina Ludwig, Ms. Sarah Lipp, Ms. Olga Trivailo,

Ms. Cecilia Valluchi, Ms. Natascha Bonidis, Mr. Alexander Kopp, Mr. Arnold van Foreest, Mr. Ryoma Yamashiro, Mr. Sven Stappert, Mr. Mete Bayrak, Mr. Magni Johannsson, Mr. David Gerson, Mr. Jochen Bütünley, Mr. Sven Krummen, Mr. Tobias Schwanekamp, Mr. Sholto Forbes-Spyratos, Mr. Marco Palli, Mr. Jan-René Haferkamp, Mr. David von Rüden and Mr. Vincent Friesen to the analyses and preliminary design of the SpaceLiner.

6 REFERENCES

1. Musk, E.: Making Life Multi-Planetary, in *NEW SPACE*, VOL. 6, NO. 1, 2018 DOI: 10.1089/space.2018.29013.emu
2. Sippel, M.; Stappert, S.; Koch, A.: Assessment of Multiple Mission Reusable Launch Vehicles, in Journal of Space Safety Engineering 6 (2019) 165–180, https://doi.org/10.1016/j.jsse.2019.09.001
3. Herberhold, M.; Bussler, L; Sippel, M.; Wilken, J.: COMPARISON OF SPACEX'S STARSHIP WITH WINGED HEAVY-LIFT LAUNCHER OPTIONS FOR EUROPE, DLRK, Hamburg 2024 and accepted for publication in CEAS-Space Journal
4. Sippel, M., Klevanski, J., Steelant, J.: Comparative Study on Options for High-Speed Intercontinental Passenger Transports: Air-Breathing- vs. Rocket-Propelled, IAC-05-D2.4.09, October 2005
5. Sippel, M., Klevanski, J., van Foreest, A., Gülhan, A., Esser, B., Kuhn, M.: The SpaceLiner Concept and its Aerothermodynamic Challenges, 1st ARA-Days, Arcachon July 2006
6. Sippel, M., Trivailo, O., Bussler, L., Lipp, S., Kaltenhäuser, S.; Molina, R.: Evolution of the SpaceLiner towards a Reusable TSTO-Launcher, IAC-16-D2.4.03, September 2016, Download Link
7. Sippel, M.; Singh, S.; Stappert, S.: Progress Summary of H2020-project FALCon, Aerospace Europe Conference 2023 – 10th EUCASS – 9th CEAS, Lausanne July 2023, Download Link
8. Sippel, M.; van Foreest, A.; Dietlein, I.; Schwanekamp, T.; Kopp, A.: System Analyses Driving Improved Aerothermodynamic Lay-out of the SpaceLiner Configuration, ESA-SP692, May 2011
9. Garbers, N.: Overall Preliminary Design of the Thermal Protection System for a Long Range Hypersonic Rocket-Powered Passenger Vehicle (SpaceLiner), ESA TPS-HS Workshop 2013
10. Sippel, M.; Schwanekamp, T.: The SpaceLiner Hypersonic System – Aerothermodynamic Requirements and Design Process, 8th European Symposium on Aerothermodynamics for Space Vehicles, Lisbon, March 2015
11. Schwanekamp,T., Garbers, N.; Sippel, M.: Conceptual Design of the SpaceLiner Thermal Protection System, 8th European Symposium on Aerothermodynamics for Space Vehicles, Lisbon 2015
12. Sippel, M.; Stappert, S.; Bussler, L.; Singh, S.; Krummen, S.: Ultra-Fast Passenger Transport Options Enabled by Reusable Launch Vehicles, 1st FAR conference, Monopoli, September 30th – October, 3rd 2019, Download Link
13. Sippel, M.; Dietlein, I.; Wilken, J.; Pastrikakis, V.; Barannik, V.; du Toit, Th.; Moroz, L System Aspects of European Reusable Staged-Combustion Rocket Engine SLME, Space Propulsion Conference, Glasgow, 20-23 May 2024, Download Link
14. Sippel, M., Stappert, S., Bayrak, Y.M.; Bussler, L.: Systematic Assessment of SpaceLiner Passenger Cabin Emergency Separation Using Multi-Body Simulations, CEAS Space Journal, Vol. 15, No. 6, November 2023, published online: 02 June 2023, https://doi.org/10.1007/s12567-023-00505-z
15. Schwanekamp, T.; Mayer, F.; Reimer, T.; Petkov, I.; Tröltzsch, A.; Siggel, M.: System Studies on Active Thermal Protection of a Hypersonic Suborbital Passenger Transport Vehicle, AIAA Aviation Conference, AIAA 2014-2372, Atlanta, June 2014
16. Reimer, T.; Rauh, C.; Di Martino, G.D.; Sippel, M.: Thermal Investigation of a Purged Insulation System for a Reusable Cryogenic Tank, Journal of Spacecraft and Rockets, 59 (4), p. 1205-1213, https://doi.org/10.2514/1.A35252
17. Rauh, C.; Reimer, T.; Sippel, M.; Wilken, J.; Liebisch, M.; Hildebrandt, B.: DLR CONCEPTS OF ADVANCED THERMAL PROTECTION SYSTEMS FOR REUSABLE CRYOGENIC PROPELLANT TANKS, 3rd FAR-conference, Arcachon, 18th-22nd May 2025
18. Tommaso Mauriello, Jascha Wilken, Steffen Callsen, Leonid Bussler, Martin Sippel, Multidisciplinary design analysis and optimization of the aerodynamic shape of the SpaceLiner passenger stage, Acta Astronautica, 2024, https://doi.org/10.1016/j.actaastro.2024.07.054
19. Mauriello, T.; Callsen, S.; Bussler, L; Wilken, J.; Sippel, M.: Multidisciplinary Design Assessment of Promising Aerodynamic Shapes for Hypersonic Passenger Transport, IAC-24-D2.4.6, 75th International Astronautical Congress (IAC), Milan, Italy, 2024, Download Link
20. Sippel, M., Wilken, J., Callsen, S.; Bussler, L.: Towards the next step: SpaceLiner 8 pre-definition, IAC-23-D2.4.2, 74th International Astronautical Congress (IAC), Baku, Azerbaijan, 2023, Download Link
21. M. Sippel, J. Wilken, L. Bussler, S. Callsen, T. Mauriello, Progress in Pre-Definition of the SpaceLiner 8 Advanced Hypersonic Transport, 3rd International Conference on High-Speed Vehicle Science Technology (HiSST), April 2024, Busan, Korea, Download Link
22. Bussler, L; Sippel, M.; von Rüden, D.F.: Reference Concept SLB 8 Booster, AKIRA report R-2004, SART TN-001/2020, March 2020
23. Callsen, S., Wilken, J., Sippel, M.: Analysis of sonic boom propagation and population disturbance of hypersonic vehicle trajectories, CEAS Space Journal. (2024) Springer. doi: 10.1007/s12567-024-00583-7.
24. Callsen, S.; Bussler, L.; Sippel, M.: AERODYNAMIC STABILITY AND SYSTEM IMPACT ANALYIS OF SPACELINER PASSENGER AND RESCUE CABIN, 3rd FAR-conference, Arcachon, 18th-22nd May 2025

Further updated information concerning the SART space transportation concepts is available at:
https://www.dlr.de/sart